Iranian Journal of Pharmaceutical Sciences
Summer 2008: 4(3): 209-216
www.ijps.ir

Original Article

Analytically Modeling of *In Vitro* Calcium Dissolution of Plasma-Sprayed Hydroxyapatite Coatings

Zahra Mohammadi[a,*], Aliakbar Ziaei-Moayyed[a], Abdorreza Sheikh-Mehdi Mesgar[a], Mohammad Hossain Afdjei[b]

[a]*Materials Science and Engineering Department, Sharif University of Technology, Tehran, Iran*
[b]*Education Group, Ministry of Health and Medical Education, Tehran, Iran*

Abstract

The *in vitro* dissolution of plasma-sprayed hydroxyapatite (PHA) coatings with different characteristics, produced by various spraying conditions, in a Tris-buffered solution at pH 7.4 was experimentally studied through the measurement of calcium ions release with Inductively Coupled Plasma Atomic Emission Spectroscopy (ICP-AES), and then modeled. Three coating characteristics, the crystallinity, the degree of recrystallization and the porosity were evaluated. The analytical modeling revealed that the calcium dissolution process was composed of two stages. The first stage was found to be both surface and diffusion controlled. The second stage was an exactly diffusion controlled dissolution. In the first stage, the solubility and dissolution rate of the PHA coatings were mainly increased with decreasing the crystallinity, and partly with increasing the degree of recrystallization and the porosity. The degree of recrystallization was found to control the dissolution rate of the PHA coatings in the second stage. It was suggested that the promotion of a rapid integration of implant to bone can be achieved by the optimization of the degree of crystallinity and recrystallization at coating surface.

Keywords: Crystallinity; Dissolution; Hydroxyapatite; Plasma spray; Porosity; Recrystallization.
Received: December 18, 2007; *Accepted:* April 7, 2008

1. Introduction

It is well known that the dissolution behavior of hydroxyapatite (HA) coatings in cellular physiologic solutions *in vitro* generally gives a guide to their biosolubility [1]. The *in vitro* dissolution of HA coatings is a comprehensive process involving the coating characteristics and the employed solution parameters [2]. The influential coating characteristics on the dissolution behavior of HA coatings include phase composition, crystallinity, porosity, surface area, residual stress, surface roughness, morphology and crystal size [3-5].

Plasma spraying as the most common method of applying HA coatings produces a mixture of various HA structures (*i.e.* unmelted, dehydroxylated (OHA),

*Corresponding author: Zahra Mohammadi, Materials Science and Engineering Department, Sharif University of Technology, Tehran, Iran.
Tel (+98)21-77606689, Fax (+98)21-77606689
E-mail: mohamadiz@yahoo.com

recrystallized) and impurity phases including calcium oxide (CaO), tetracalcium phosphate (TTCP), α- and β-tricalcium phosphate (TCP), as well as amorphous calcium phosphate (ACP) [6]. The solubility of all these additional phases and structures formed in spraying are higher than HA [3, 4].

The dissolution behavior of HA coatings has been usually studied using the buffered or unbuffered solutions through the measurement of released calcium and/or phosphate concentrations with time [7, 8]. Among the various solutions, two kinds of the buffered physiologic solutions, Simulated Body Fluid (SBF) and Tris-HCl buffer, have been commonly used to study of the dissolution and mineralization processes [2-4,7-9]. The HA coatings first dissolve and then mineralized subsequently when they immersed in both of these buffered solutions [2, 7-9]. It is reported that the calcium dissolution behaviors of the HA coatings in Tris-HCl buffer are similar to those in SBF [2, 9].

The concentrations of calcium ion always increase with time in the dissolution stage [2, 7-9]. This implies that the study of the dissolution process of PHA coatings can be conducted in a much simpler buffered solution such as Tris-HCl buffer by the analysis of calcium ions release. In this work, the experimental and analytical studies were conducted to investigate the calcium dissolution of PHA coatings in Tris-buffered solution.

2. Materials and methods

Plates of Ti-6Al-4V alloy (ISO 5832-3) with the dimensions of 13×13×2 mm used as substrates were degreased with a dilute acid, grit-blasted with Al_2O_3 grit, air-blasted and cleaned with alcohol. The grit-blasted surfaces had an average surface roughness (R_a) of 3.51 μm [10]. The plasma spray parameters were described elsewhere [11].

The powder was sprayed using a METCO 3MB plasma spray system. Nine different samples of HA coatings were prepared by adjusting the input power level and the spray distance (Table 1). HA coatings with an average thickness of 200±20 μm were deposited on the roughened substrates. In order to evaluate the crystallinity and the porosity of the coatings, the HA coatings were deposited on lightly grit-blasted substrates to peeling off the coatings easily.

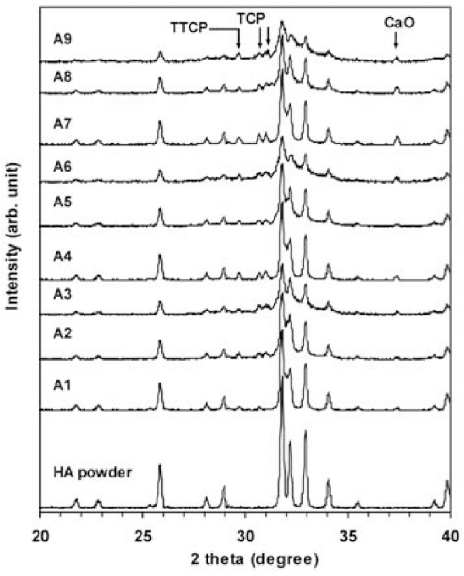

Figure 1. XRD patterns of the surface of the PHA coatings.

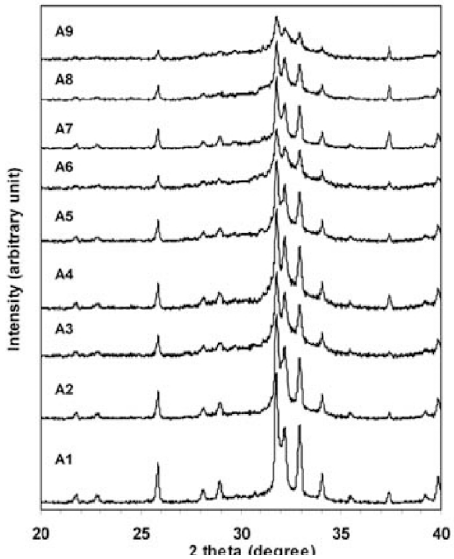

Figure 2. XRD patterns of the interface of the PHA coatings.

The coating surfaces and interfaces were examined by the X-ray diffraction (XRD) technique, using a PW3710 diffractometer with a Cu k_α radiation at a rate of 0.02 °/s. 2θ scanning was done between 20 and 40 degrees.

The crystallinity was evaluated from the main peak ratio, I/I_{HA}, base on a relative method [11], where I is the main peak height of HA on the XRD pattern of the coating at the surface or interface and I_{HA} is the main peak height of HA on the XRD pattern of the powder. The HA powder considered as a material of 100% crystallinity. The degree of crystallinity (DOC) was defined as follows:

$$\text{DOR (\%)} = (\text{IHA}) \times 100 \qquad \text{Equation (1)}$$

This method was also used to estimate the relative percent of the impurity phases of coating surface.

The degree of recrystallization at the coating surface (DOR) was estimated by comparing the difference of the crystallinity at the coating surface ($[DOC]_S$) and interface ($[DOC]_I$) [6]:

$$\text{DOR (\%)} = [\text{DOC}]_s - [\text{DOC}]_1 \qquad \text{Equation (2)}$$

Porosity of the peel-off coatings was measured by using Archimedean method based on the procedure suggested by Mancini *et al*. [12]. Three samples were tested for each condition.

The HA coatings deposited on the roughened substrates were used in the dissolution experiments. The evaluation of dissolution behavior was made by measuring the concentration of calcium ion released into the Tris-HCl buffer solution at 37 °C for 0.5, 1, 4, 8, 24, 48, 72 and 120 h using Inductively Coupled Plasma Atomic Emission Spectroscopy (ICP, ARL 3410). Tris-HCl buffer solution (pH 7.4) was prepared using 0.5 M tris-hydroxymethyl-aminomethane and 0.5 M HCl. Two dissolution experiments were done for each condition.

3. Results and discussion

3.1. Characterization of the coatings

The XRD patterns of the HA powder and the HA coatings at surfaces are shown in Figure 1. It reveals that the feedstock powder is a high purity HA, meanwhile, the HA coatings are mainly composed of HA and impurity phases. The high temperature of plasma flame transformed the crystalline HA into a mixture of HA and several kinds of phases (*i.e.* TCPs, TTCP, CaO, ACP). Figure 2 shows the XRD patterns of the coatings at the interface. In both Figures 1 and 2, when either the spray power or spray distance was increased, the intensity of HA peaks decreased. In addition, the intensity of HA peaks is higher in the XRD patterns of the surface than that of the same coating interface.

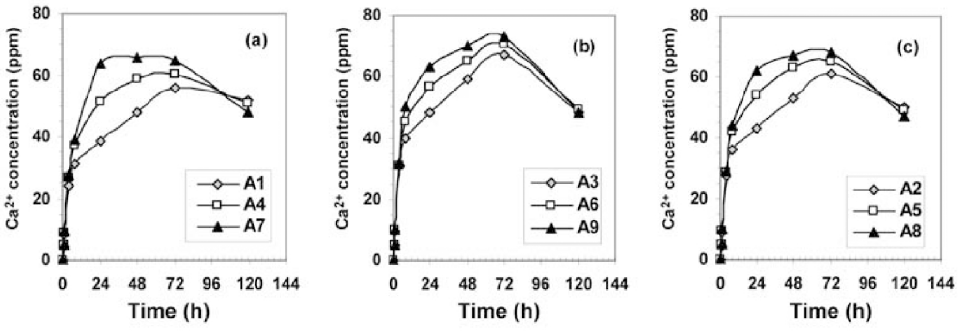

Figure 3. Calcium ion concentration (ppm) as a function of time (h) in Tris-buffered solution for the dissolution of the PHA coatings sprayed at three different plasma power levels and spray distance of (a) 8 cm (b) 11 cm (c) 14 cm.

Table 1 also shows the degree of crystallinity of the all HA coatings at the surface and the interface. It indicates that the crystallinity decreased with increasing the spray power and SD. In general, more melting of the particles and higher cooling rate of the melted particles lead to form much more ACP, and thus decrease of the crystallinity. As can be seen in Table 1, the crystallinity at the interface was lower than that of the same coating surface. This difference can be attributed to the different degree of recrystallization. During spraying, the HA particles may be melted and/or dehydroxylated. The melted particles can either solidify to ACP, recrystallized, or decompose to impurity phases. On the other hand, the dehydroxylated portions will transform into OHA. Under spraying conditions used in this work, it is reported that the identified HA by XRD is mostly OHA [15].

The apparent porosity percent of the samples were mostly consistent with the results of the crystallinity at coating surface; *i.e.* the lower the crystallinity, the lower the porosity (Table 1). The formation of more amorphous phase due to an increase of spray power and/or SD gives rise to better filling of the pores between splats and decrease of the porosity.

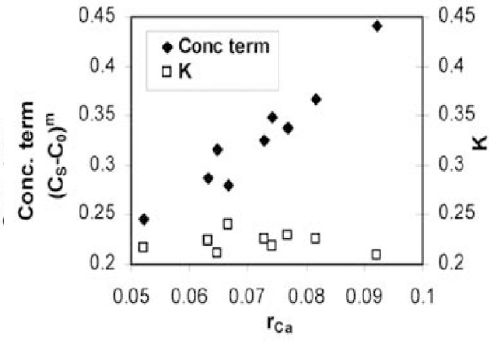

Figure 4. Dissolution rate of calcium ions in the first stage of the dissolution process (r_{Ca}) for the PHA coatings plotted against its constituents, concentration term and dissolution parameter (K).

3.2. Dissolution study and the modeling

Figure 3 showed the calcium concentration changes in the Tris-buffered solution during 5 days immersion. All of the coatings, except coating A7, first dissolved after 3 days immersion and then mineralized subsequently as a result of a decrease in calcium concentration after 5 days incubation in the solution. Dissolution occurred in the coating A7 before 2 days immersion in the solution.

In order to correlate between coating characteristics and calcium ion release, it is attempted to fit the dissolution curves with the mathematical functions. As can be observed from Figure 3, the trends of calcium concentration changes with time can be divided into the two stages. In the first stage, the calcium release rapidly increases with time. After this stage, the increase in calcium concentrations with time is continued with a lower rate compared to the previous stage. This indicated that two functions had to be used to fit the dissolution curves. The experimental point (t_s, C_s) calls the point that separates the two analytical functions. This point should be chosen for each curve so that both suggested functions have the best R^2.

In the first stage, the dissolution process could be fitted with the following function:

$$\text{Ln}\,(C_s - C_0) = \text{Ln}\,x + y\text{In}\,t \qquad \text{Equation (3)}$$

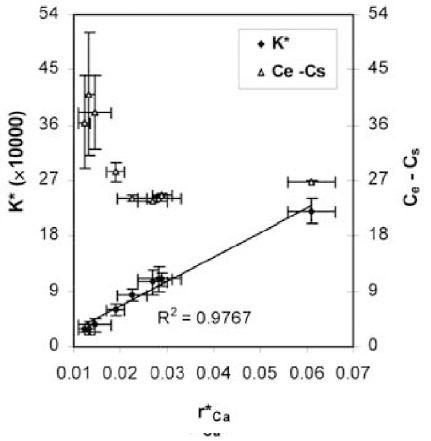

Figure 5. Dissolution rate of calcium ions in the second stage of the dissolution process (r^*_{Ca}) for the PHA coatings plotted against its constituents, concentration term and dissolution parameter (K*).

where C was the calcium concentration in the solution, t was the time, and x and y were the parameters. The rate of dissolution in this stage (r) can be described by the equation:

$$r_{Ca} = K(C_s - C_0)^m \qquad \text{Equation (4)}$$

where K is the dissolution parameter which can be influenced by the physical characteristics of the coating such as specific area, C_s is the calcium concentration after the incubation time of ts in the solution, C_0 is the initial concentration which was taken as the calcium release after 0.5 h immersion in the solution, and m is the effective order of reaction. The K and m in the Equation 4 are different functions of x and y in the Equation 3.

A simple diffusional model was chosen to try fitting the second part of the dissolution process based on the following equation:

$$\ln\left(\frac{C_e - C_s}{C_e - C}\right) = K^*(t - t_s) \qquad \text{Equation (5)}$$

where C_e represents the equilibrium concentration and K^* was the dissolution parameter in the second stage. The equation describes the dissolution rate in the second stage (r^*_{Ca}):

$$r^*_{Ca} = K^*(C_e - C_s) \qquad \text{Equation (6)}$$

The first step in the modeling was to choose the time t_s from the experimental results so that the equations and had the highest R^2. The fitting of the curves with a value of t_s = 8 h led to obtain the best R^2 for both functions in the range of 0.96-0.998. Using this value of t_s, the x and y parameters in the function describing the fist stage of the dissolution process (*i.e.* Equation 3) could be obtained for each coating. The C_e values for each coating were estimated by fitting of the curves based on the Equation 5 pass through the experimental points in the second stage of the dissolution. Table 2 shows the values of x, y and C_e obtained for each of the HA coatings. Using these values, the other parameters (*i.e.* K, m and K^*) which were necessary to calculate the rates of dissolution could be easily obtained. We call t* the time necessary to reach a stationary state which is assumed to be a required time to dissolve an amount of calcium ions corresponding to the 0.99 % of C_e (see Table 2).

Table 2 shows that the values of parameters y for all PHA coating change in the range of 0.71-0.83. It is noted that a diffusion-controlled dissolution process would require a value y=0.5. The dissolution models of calcium apatites reviewed by Dorozhkin [13]. Several models are suggested to describe the

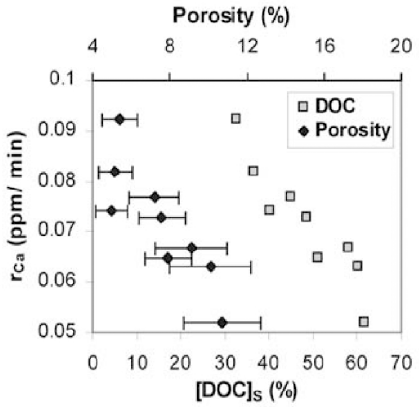

Figure 6. Correlation of the dissolution rate in the first stage of the dissolution process (r_{Ca}) for the PHA coatings with their porosity levels and crystallinity at surface ($[DOC]_S$).

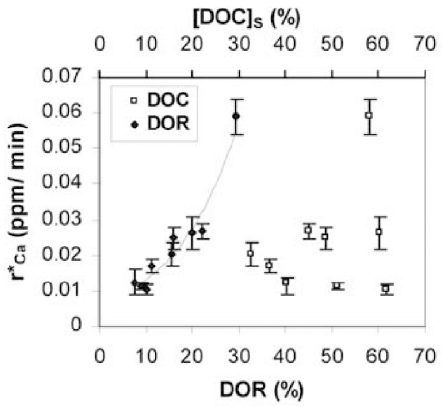

Figure 7. Correlation of the dissolution rate in the second stage of the dissolution process (r^*_{Ca}) with the crystallinity at surface ($[DOC]_S$) and the degree of recrystallization (DOR) for the PHA coatings.

Table 1. Plasma spraying conditions and characteristics of the coatings.

Spraying condition			Coating characteristic					
Coating	Power	SD	$[DOC]_s$	[DOC]I	Porosity	CaO	TCP	TTCP
	(kW)	(mm)	(%)	(%)	(%)	(%)	(%)	(%)
A1	28.0	80	61.7	51.7	10.7±2.0	2.9	6.2	3.6
A2	28.0	110	51.2	42.2	7.9±1.2	2.2	6.8	3.1
A3	28.0	140	40.3	32.6	5.0±0.8	2.1	7.5	2.5
A4	32.2	80	60.1	40.1	10.1± 2.1	3.2	12.5	6.5
A5	32.2	110	48.7	32.8	7.6±1.2	3.1	12.6	6.2
A6	32.2	140	36.5	25.1	5.2±0.9	3.2	12.2	6.7
A7	36.4	80	58.1	28.7	9.1±1.9	6.8	18.1	6.2
A8	36.4	110	45.1	23.0	7.2±1.3	5.4	18.3	7.3
A9	36.4	140	32.5	17.0	5.4±0.9	4.9	18.0	8.6

dissolution process of calcium apatites, which are valid within the experimental conditions studied only. Among the models, the diffusion and surface controlled models could elaborate the dissolution process of apatite in nearly neutral and undersaturated solutions. It is believed that the solution immediately next to the coating surface is undersaturated with respect to the apatite in the surface controlled process and this solution is saturated in the diffusion-controlled process [13]. The driving force is a gradient of ionic chemical potentials between the coating surface and bulk solution in the former, and a concentration gradient within the Nernst diffusion layer in the latter. The obtained values of parameter y (*i.e.* higher than 0.5) and the fact that the dissolution experiments in this study were conducted without stirring the solution indicate the calcium dissolution process of the PHA in the Tris-buffered solution under conditions used in this study was both kinetically (surface) and diffusion controlled.

To analyze the results, the effect of influential constituents of dissolution rate in each stage (*i.e.* the parameters K and K^* and concentrations term in equations 4 and 6 on the magnitude of the rates was taken into account. The relationship between the dissolution rate and the influential constituent in each of the dissolution stages are shown in Figures 4 and 5. Figure 4 shows that there is an approximately direct relationship between concentration difference and the calcium dissolution rate in the first stage of the dissolution stage. On the contrary, the calcium dissolution rate in the second stage of the dissolution stage is directly dependent on the parameter K^*.

It is believed that the solubility of the all phases found in the PHA coatings in the SBF is in the order of CaO >> TCP > ACP > TTCP > OHA >> HA [7]. The recrystallized portions of the PHA coatings is mainly composed of nanocrystals with much greater interfacial volume as well as defect point compared to crystalline HA, which tends to the their high solubility [4]. If the above trend is true for the immersion of the PHA coatings in the Tris-buffered solution, it is expected that the PHA coatings with a higher amount of impurity phases (especially CaO and TCP) show a higher solubility, and therefore a higher value of r_{Ca} as a result of more influential effect of concentration difference on the dissolution rate in the first stage of the dissolution process.

We could not find a meaningful relationship between the relative percents of CaO and/ or TCP and the values of r_{Ca}. However, the rCa values of the PHA coatings were linearly changed with crystallinity of the coating surface ($[DOC]_S$) in approximate, as seen in Figure 6. This indicated that the solubility and the rate of calcium dissolution in the initial times of the immersion are primarily controlled by the crystallinity of the coating.

Figure 5 shows a linear relationship between the dissolution rate of the PHA

Table 2. Parameters for calcium dissolution obtained from fitting the experimental data.

Coating	x	y	Ce	t*
A1	0.43	0.71	65.0±5.0	259±89
A2	0.38	0.76	74.0±7.0	258±90
A3	0.37	0.78	77.5±5.5	236±102
A4	0.41	0.74	60.9±0.4	66±11
A5	0.39	0.77	66.0±0.6	67±9
A6	0.37	0.79	73.0±1.1	113±19
A7	0.43	0.74	65.8±0.1	37±3
A8	0.39	0.78	68.5±0.3	63±5
A9	0.32	0.83	74.0±0.4	79±13

coatings in the second part of the dissolution process and the parameter K^*. This indicates that the difference in the dissolution rates of the PHA coatings can be attributed to the different values of K^*. Since the conditions of dissolution tests for the PHA coatings were the same, the difference in the values of K^* could be caused by the difference in those coating characteristics which influence the surface area of the coatings. Figure 7 exhibits the importance of the degree of recrystallization (DOR) on the rate of dissolution in the second stage of the dissolution process (r^*_{Ca}) so that the r^*_{Ca} values of the PHA coatings increase with increasing their DOR values.

It is suggested that the short-term release of ions from dissolving calcium phosphate phases must be optimized [7]. The results of this study indicated that even in the presence of impurity phases, the difference in the solubility and dissolution rate of the PHA coatings at initial times of immersion (*i.e.* 8 h) are mainly attributed to the difference in the crystallinity of coating surface, and partly to the difference in their porosity levels and amounts of recrystallized HA. On the other hand, the releasing rate of calcium ions from the PHA coatings at longer times, as well as the required time to reach the stationary state (i.e. t^*) which after that the mineralization process will be dominant, were mainly dependent to their amounts of recrystallized HA. On the base of these findings, one may be suggested to promote a rapid integration of the PHA coatings, their degrees of crystallinity and recrystallization at surface should be optimized.

4. Conclusions

The dissolution of the PHA coating was describes by two functions. The first stage of the dissolution process (up to 8 h) was modeled by a power-law function and the second stage with a simple diffusion function. The dissolution of the PHA coatings in the first stage was found to be both surface and diffusion controlled. In the first stage, the solubility and dissolution rate of the PHA coatings were mainly increased with decreasing the crystallinity, and partly with increasing the degree of recrystallization and the porosity. The degree of recrystallization was found to control the dissolution rate of the PHA coatings in the second stage. It was suggested that the promotion of a rapid integration of implant to bone can be achieved by the optimization of the amounts of recrystallized HA and ACP at coating surface.

References

[1] Tsui YC, Doyle C, Clyne TW. Plasma-sprayed hydroxyapatite coatings on titanium substrates Part 2: Optimization of coating properties. *Biomaterials* 1998; 19: 2031-43.

[2] Zhang Q, Chen J, Feng J, Cao Y, Deng C, Zhang X. Dissolution and mineralization behaviors of HA coatings. *Biomaterials* 2003; 24: 4741-8.

[3] Radin SR, Ducheyne P. Plasma spraying induced changes of calcium phosphate ceramic characteristics and the effect on *in vitro* stability. *J Mater Sci Mater Med* 1992; 3: 33-42.

[4] Sun L, Berndt CC, Khor KA, Cheang HN, Gross KA. Surface characteristics and dissolution behavior of plasma-sprayed hydroxyapatite coating. *J Biomed Mater Res* 2002; 62: 228-36.

[5] Sergo V, Sbaizero O, Clarke DR. Mechanical and chemical consequences of the residual stresses in plasma-sprayed hydroxyapatite coatings.

Biomaterials 1997; 18: 477-82.

[6] Sun L, Berndt CC, Grey CP. Phase, structural and microstructure investigations of plasma sprayed hydroxyapatite coatings. *Mater Sci Engineering A* 2003; 360: 70-84.

[7] Grafmann O, Heimann R. Compositional and micro-structural changes of engineered plasma-sprayed hydroxyapatite coatings on Ti6Al4V substrates during incubation in protein-free simulated body fluid. *J Biomed Mater Res* 2000; 53: 685-93.

[8] Mohammadi Z, Ziaei-Moayyed AA, Sheikh-Mehdi Mesgar A. *In vitro* calcium dissolution behavior of hydroxyapatite coatings with different characteristics. *Cairo International Biomedical Engineering Conference IEEE* 2006.

[9] Mohammadi Z, Ziaei-Moayyed AA, Sheikh-Mehdi Mesgar A. Dissolution behavior of plasma sprayed hydroxyapatite coatings in simulated body fluid and Tris-buffer Solution. *10th Iranian Metallurgy Engineering Society* 2006.

[10] Mohammadi Z, Ziaei-Moayyed AA, Sheikh-Mehdi Mesgar A. Grit blasting of Ti-6Al-4V alloy: Optimization and its effect on adhesion strength of plasma-sprayed hydroxyl-apatite coatings. *J Mater Proc Tech* 2007.

[11] Mohammadi Z, Ziaei-Moayyed AA, Sheikh-Mehdi Mesgar A. Adhesive and cohesive properties by indentation method of plasma-sprayed hydroxyapatite coatings. *Appl Surface Sci* 2007; 253: 4960-5.

[12] Mancini CE, Berndt CC, Sun L, Kucuk A. Porosity determinations in thermally sprayed hydroxyapatite coatings. *J Mater Sci* 2001; 36: 3891-6.

[13] Dorozhkin SV. A review on the dissolution models of calcium apatites. *Prog Cryst Growth Charact Mater* 2002; 44: 45-61.